

EFFECT OF HEAT REJECTION CONDITIONS ON CRYOCOOLER OPERATIONAL STABILITY

R.G. Ross, Jr. and D.L. Johnson

Jet Propulsion Laboratory
California Institute of Technology
Pasadena, CA 91109

ABSTRACT

It is well known that cryocooler thermal efficiency is a strong function of heat rejection temperature, roughly following the dependency described by Carnot. An equally important and generally overlooked implication of cryocooler heat-rejection thermodynamics is the effect of the heat rejection temperature control mode on cryocooler performance and operational stability. Example heat rejection temperature control modes include constant reject temperature (generally maintained via closed-loop temperature control), heat rejection temperature rising linearly with power dissipation (typical of conduction/convection to a constant temperature heat sink), and heat rejection dependent on the fourth power of reject temperature (typical of radiation to deep space). This paper presents a useful algorithm for computing the effect of changing heatsink temperature on cryocooler performance and uses the algorithm to examine the implications of various heat rejection temperature control modes on cryocooler operation. A useful system-level thermal performance map is developed to display the stability boundaries and available stable operating space for coolers of interest for various typical heat rejection control modes.

INTRODUCTION

Increasing numbers of space instruments are using mechanical cryocoolers to enable improved scientific measurements to be made via cryogenically cooled infrared, submillimeter and gamma-ray detectors. One example is JPL's Atmospheric Infrared Sounder (AIRS) instrument, which uses a 55K cryocooler with closed-loop temperature control to maintain the HgCdTe focal plane at 58 K throughout the mission lifetime. The complete cryocooler system includes heat rejection to spacecraft-mounted radiators via a system of conductive elements and heatpipes.¹ Of particular interest is the overall thermal performance and closed-loop stability of the complete cryocooler system including the heat rejection subsystem.

To achieve the necessary understanding of overall thermal performance and closed-loop stability it is first necessary to accurately quantify the dependency of cryocooler performance on heatsink temperature. This has been done for a wide variety of coolers by characterizing their operational performance over an extensive operating range using the

techniques developed at JPL for general cryocooler characterization.' Next, a special parametric performance plot has been developed to display the measured performance including temperature dependency, and used to note the stability boundaries and available stable operating space for the cooler with a given heat-rejection temperature control mode.

For this paper, the analysis originally done for AIRS has been generalized to provide a universal approach to examining cryocooler heatsink temperature sensitivity and operational stability boundaries. To demonstrate the techniques, data are presented for various typical heat rejection temperature control modes including constant-temperature, conduction-dominated, and radiation-dominated operation.

PERFORMANCE SENSITIVITY TO HEATSINK TEMPERATURE

Following the dependency described by Carnot, i.e.

$$COP_{Carnot} = T_c / (T_h - T_c) \tag{1}$$

where T_c is the cryogenic temperature and T_h is the heatsink temperature, it is well known that cryocooler thermal efficiency is a strong function of heat rejection temperature. To analyze the thermal performance and stability implications of various cryocooler heat-rejection systems, it is necessary to first accurately quantify the actual temperature dependency of non-ideal operational cooler performance and to reduce the dependency to equation form, if possible. One means of accomplishing this is to examine overall cryocooler thermal performance dependency with respect to the principal operational variables exclusive of heatsink temperature, and then to note the change specifically associated with change in heatsink temperature. For the purposes of this paper, the TRW 3503 pulse tube cooler and the STC 80K Stirling cooler are used as examples.^{3,4}

Figure 1 describes the general parameter dependency of Stirling and pulse tube cooler performance on input power, refrigeration load, refrigerant ion temperature, and compressor piston stroke — all for a heatsink temperature of 20°C; these particular data are for the TRW 3503 pulse tube cooler. Next, Fig. 2 displays the shift in the cooler performance caused by

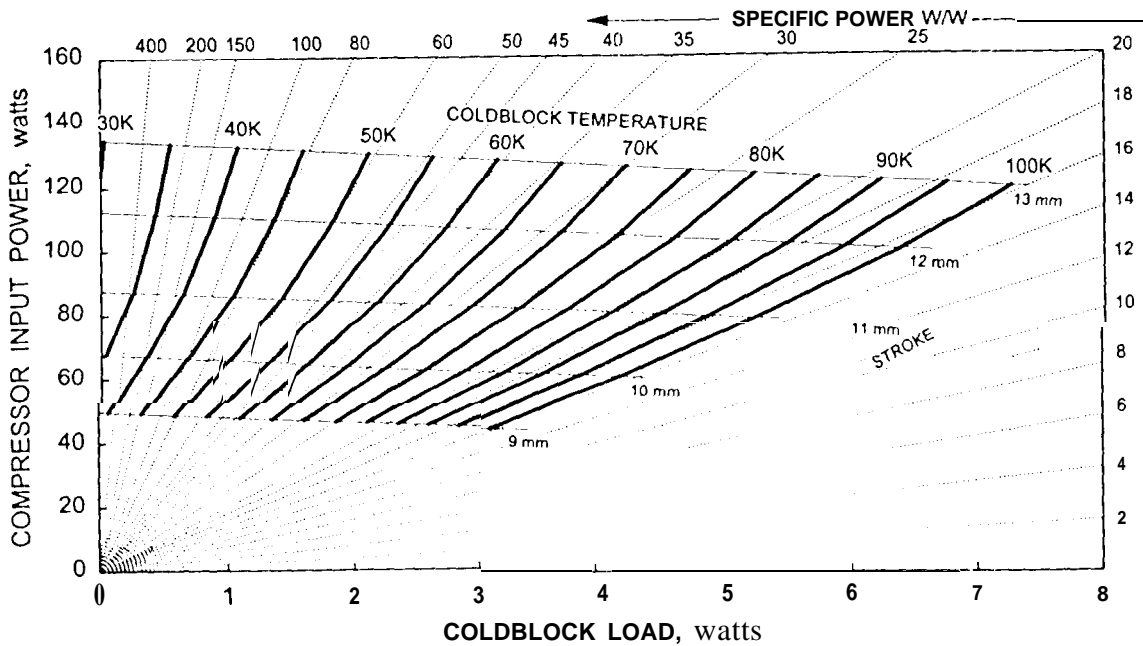


Figure 1. Measured thermal performance of the TRW 3503 pulse tube cooler with a 20°C heat rejection temperature

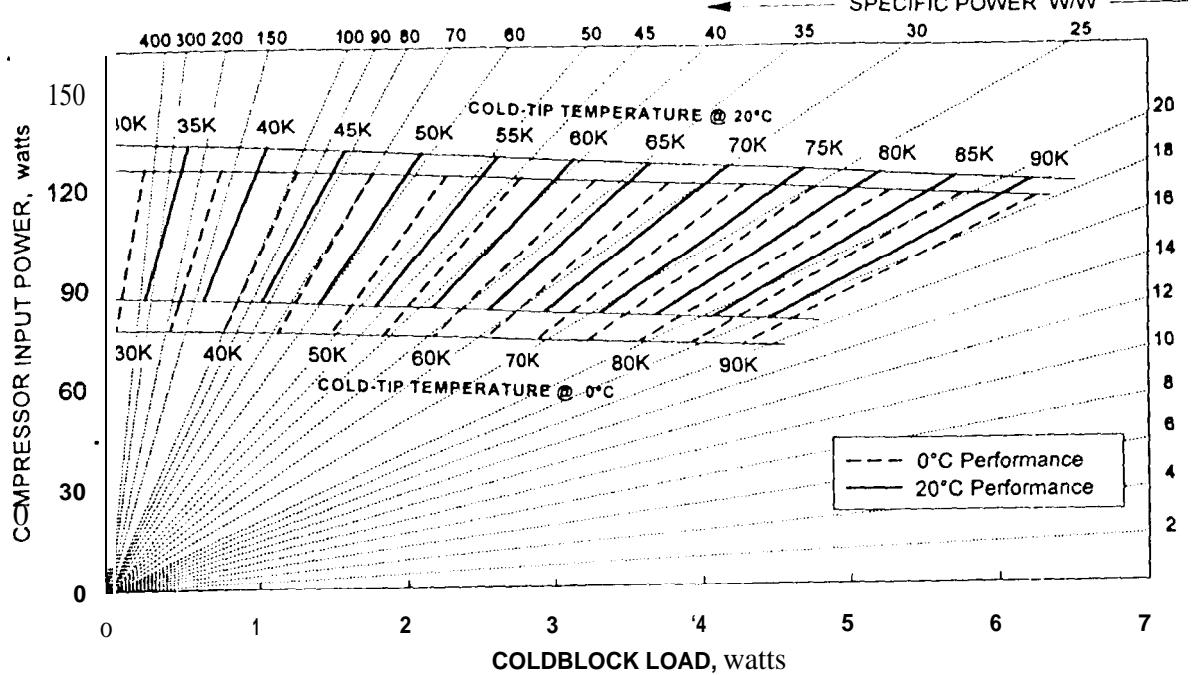


Figure 2. Measured sensitivity of thermal performance of the TRW 3503 pulse tube cooler to a change in heat rejection temperature from 20°C to 0°C.

lowering the heatsink temperature to 0°C. Note that the new isotherms (lines of constant refrigeration temperature) for a 0°C heatsink temperature are positioned on top of similar 20°C-isotherms corresponding to refrigeration temperatures approximately 3 K warmer; i.e. the performance at 55 K with a 0°C heatsink temperature is the same as the performance at 58 K with a 20°C heatsink temperature. Note that this shift is quite constant over the complete range of refrigeration temperatures plotted, from no-load on up. This fixed change in coldtip temperature per change in heatsink temperature has been found to be approximately true for a wide variety of cryocoolers, not just the TRW 3503 pulse tube.^{2,3,5} However, the proportionality constant (\mathfrak{R}) between heatsink temperature and coldend temperature varies modestly from cooler to cooler. As noted in Table 1, values of \mathfrak{R} measured at JPL range from 2 to 10 °C/K. As an example of a higher sensitivity to heat sink temperature, Fig. 3 shows the 3.5 °C/K performance of the STC Stirling cooler.

Table 1. Change in heatsink temperature required to cause a 1 K shift in coldend temperature for typical Stirling and pulse tube cryocoolers.

Cryocooler Model	Heatsink Temperature Change Coldend Temperature Shift \mathfrak{R} (°C/K)
TRW 1W-35K Pulse Tube	6
TRW 3503 Pulse Tube	7
TRW 6020 Pulse Tube	5
STC 80K Stirling	3.5
Sunpower 140K Stirling	2
MMS 80K Stirling	4
MMS 50-80K Stirling	4-10

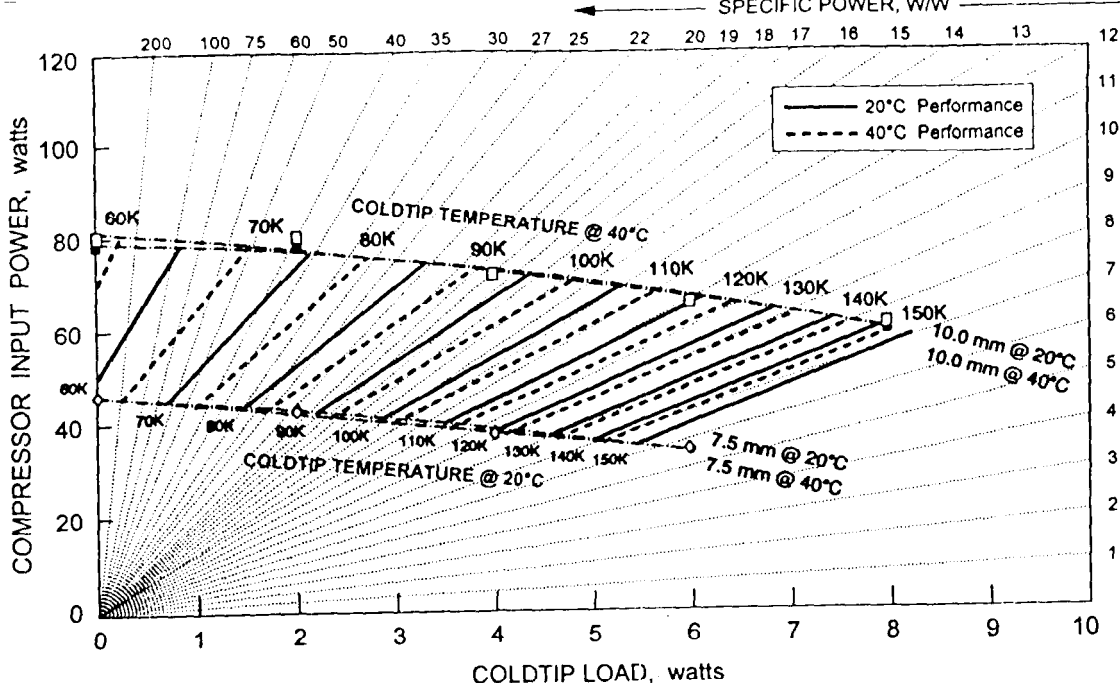


Figure 3. Measured sensitivity of thermal performance of the 80K STC Stirling cooler to change in heat rejection temperature from 20°C to 40°C.

Based on this empirically derived finding, one can construct the following algorithm for computing the refrigeration performance P at coldend temperature K and heatsink temperature T_2 in terms of the performance of the same refrigerator at a baseline heatsink temperature T_1 , i.e.

$$P_{T_2}(K) = P_{T_1}(K) \frac{(T_2 - T_1)}{\mathfrak{R}} \quad (2)$$

where \mathfrak{R} is the measured change in heatsink temperature required to shift the coldend performance by 1 K. Equation (2) allows a performance plot such as Fig. 1 to be used to determine refrigeration performance for a range of heatsink temperatures (T_2) different from the measuring conditions (T_1) for which the plot was constructed.

As an example, consider the change in input power and compressor stroke required to maintain a 1.5 watt cryogenic load at 55 K with the TRW 3503 cooler when the heatsink temperature changes from 20°C to 40°C. Using Eq. (2) with $\mathfrak{R} = 7 \text{ }^\circ\text{C/K}$, yields

$$P_{40}(55) = P_{20}\left(55 - \frac{(40 - 20)}{7}\right) = P_{20}(52.2) \quad (3)$$

As displayed in Fig. 4, which is a replot of Fig. 1, one finds that the power increases from 72 watts to approximately 82 watts, and the stroke increases from approximately 10.3 mm to 10.8 mm.

As a second example, Fig. 4 also notes the change in input power and compressor stroke required to maintain the 1.5 watt cryogenic load at 55 K when the heatsink temperature increases to 60°C. The corresponding calculation using Eq. (2) is

$$P_{60}(55) = P_{20}\left(55 - \frac{(60 - 20)}{7}\right) = P_{20}(49.3) \quad (4)$$

Thus, performance at 55 K with a 60°C reject corresponds to performance to 49.3 K with a 20°C reject.

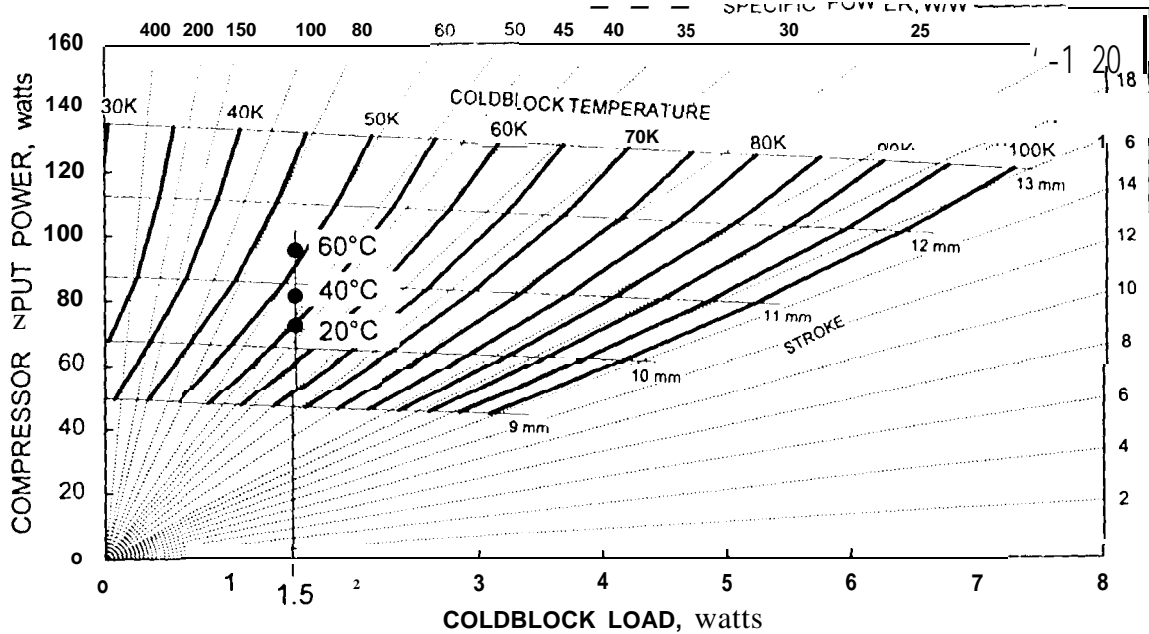


Figure 4. Example computation of the effect of changing the heatsink temperature from 20°C to 40°C and 60°C on the input power required to maintain a load of 1.5 watts at 55 K.

This strong coupling between heatsink temperature and cryocooler performance, as noted in Fig. 4, draws attention to the important role of the cryocooler’s heat rejection system and its temperature control mode.

IMPLICATIONS OF CRYOCOOLER TEMPERATURE-CONTROL MODE

Example heat rejection temperature control modes include constant reject temperature (generally maintained via closed-loop temperature control), heat rejection temperature rising linearly with power dissipation (typical of conduction/convection to a constant-temperature heatsink), and heat rejection temperature dependent on the fourth root of power dissipation (typical of radiation to deep space). Any mode other than constant heatsink temperature can significantly alter the performance attributes of the cooler as mapped in Fig. 1, and can raise the possibility of thermal runaway, whereby increased input power required at elevated heatsink temperatures further increases the heatsink temperature in an unstable spiral until maximum cryocooler stroke is exceeded.

System-level Cooler Performance Plot

To understand the system-level thermal implications of the cryocooler’s operation it is necessary to analyze not just the cryocooler by itself, but the complete cryocooler system including its heat rejection system. An effective means of accomplishing this is to note that the vertical axis of the parametric performance plot shown in Fig. 1 is power dissipation, and power dissipation, for a given heat-rejection temperature control system, directly determines the heatsink temperature. Thus, for a given heat-rejection temperature control system, one can modify the parametric performance plot to include the corresponding heatsink temperature for each compressor input power on the vertical axis. Going further, Eq. (2) can be used to re-map the cryocooler performance data for the specific heatsink temperature associated with each vertical position on the plot. The result is a system-level parametric plot of cooler performance for the given heat rejection system, as opposed to for a fixed heatsink temperature, as was done in Fig. 1.

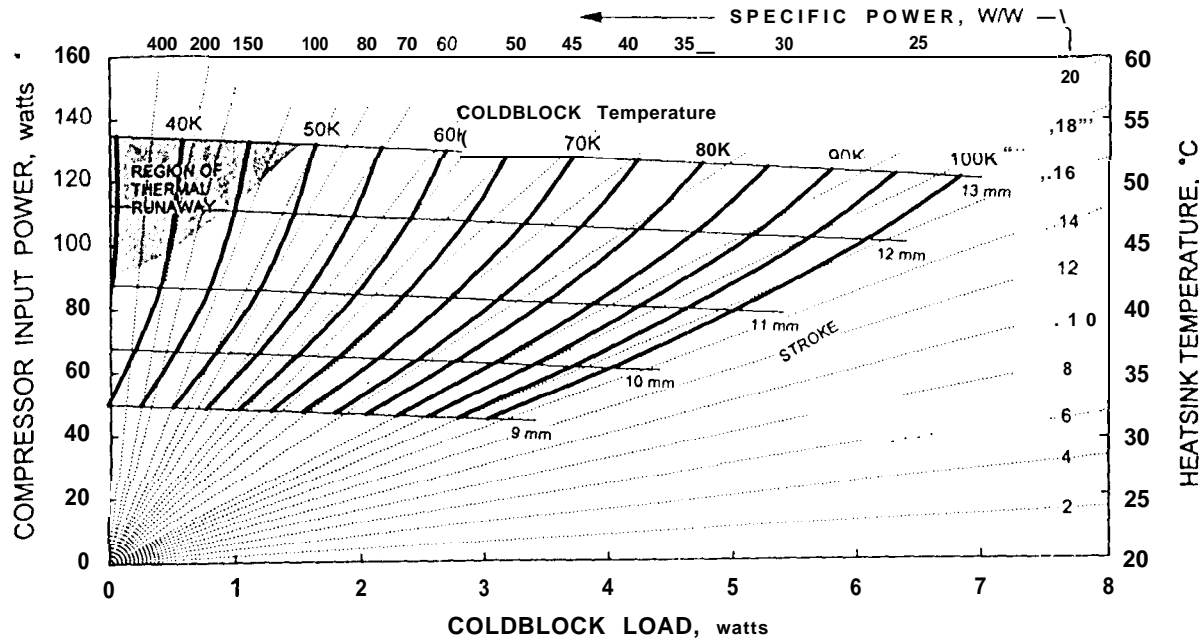


Figure 5. System-level performance of the TRW 3503 pulse tube cooler with a heatsink temperature defined by $T = 20^{\circ}\text{C} + P/4$, where P is the compressor input power in watts.

Conductive Heat Transfer. For a condition where the cooler is coupled to a constant-temperature sink through a constant-resistance thermal link, the cryocooler temperature will increase linearly above the sink temperature with increased power dissipation (P). An example would be the operation of a cooler in a constant-temperature room-ambient environment with conductive and convective heat transfer to the room.

To understand the implications of such an environment on the TRW 3503 cooler, Fig. 5 is a system-level plot based on Fig. 1, with the heatsink temperature defined by:

$$T_2 = 20^{\circ}\text{C} + P/4 \quad (5)$$

where P is the cooler input power in watts. For this heat-rejection system the cooler heatsink temperature rises linearly from 20°C to 45°C when the compressor input power increases from 0 to 100 watts. This is representative of a fairly typical bench-top test condition.

Note that the increasing reject temperature with increased input power results in the isotherm lines bending toward the upper left as compared to those for the constant 20°C heatsink temperature shown in Fig. 1. Where the isotherm lines approach a vertical slope defines the onset of thermal runaway. At this point, an attempt to serve an increased cooling load results instead in increased heating and no improvement in refrigeration capacity.

To examine the effect of different \mathfrak{R} values, Fig. 6 is a re-plot of Fig. 5 using Eq. (2) and $\mathfrak{R} = 3.5 \text{ OC/K}$ (corresponding to the temperature sensitivity of the STC 80K Stirling cooler) instead of $\mathfrak{R} = 7^{\circ}\text{C/K}$, as was measured for the TRW 3503 cooler. Note the increased bending over of the performance at higher power levels, and the larger thermal-runaway keepout region associated with this performance degradation at higher temperatures.

Radiation Heat Transfer. For a condition where the cooler is directly coupled to deep space using a high-conductivity radiator, the cryocooler absolute temperature will increase roughly proportional to the fourth root of the power dissipation, i.e. $P \propto \Theta^4$, where Θ is the absolute heatsink temperature in Kelvin.

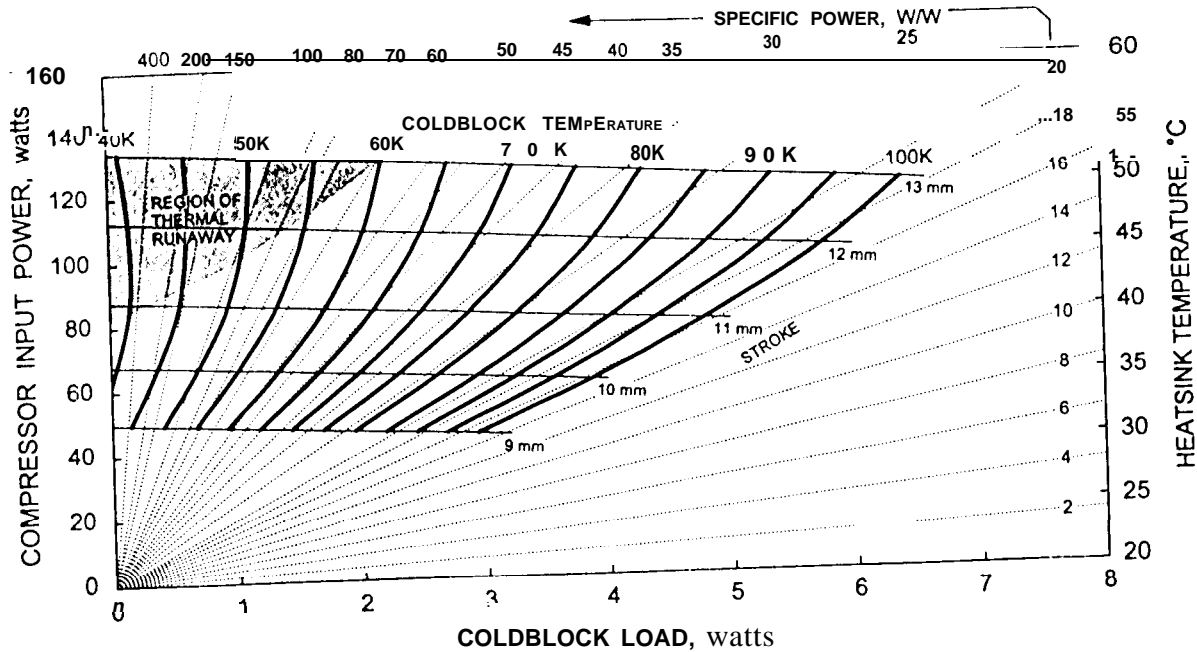


Figure 6. System-level performance of the TRW 3503 pulse tube cooler if it were to have a temperature sensitivity of $\mathfrak{R} = 3.5$ (instead of its measured $\mathfrak{R} = 7$) and a heatsink temperature defined by $T = 20^{\circ}\text{C} + P/4$, where P is input power in watts.

As an example, Fig. 7 presents the system-level performance plot for the TRW 3503 cooler for a system where the heatsink temperature is defined by:

$$T_2(^{\circ}\text{C}) = 318 (P/100)^{0.25} - 273 \tag{6}$$

i.e., the cooler absolute heat-rejection temperature rises proportional to $P^{0.25}$, reaching 318 K (45 °C) when the compressor input power reaches 100 watts. This is representative

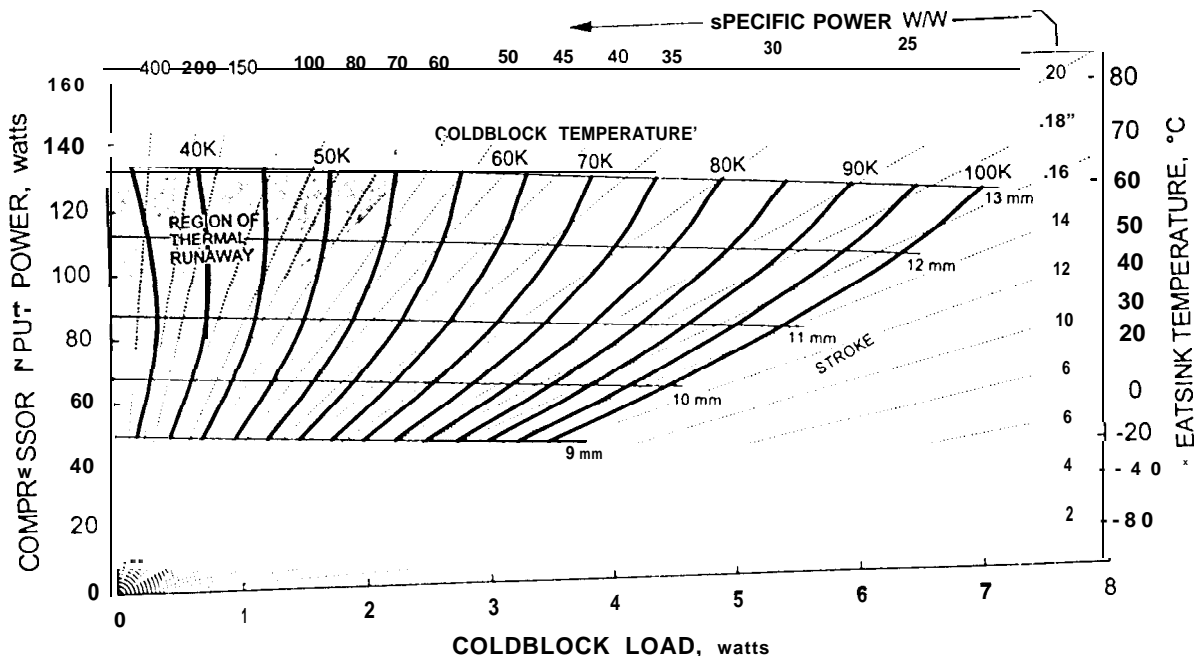


Figure 7. System-level performance of the TRW 3503 pulse tube cooler with a radiatively coupled heatsink temperature defined by $T(^{\circ}\text{C}) = 318 (P/100)^{0.25} - 273$, where P is compressor input power in watts

of many spacecraft applications.

Note that the sharply increasing reject temperature with increasing input power results in the isotherm lines bending extensively toward the upper left as compared to those for the constant 20°C heatsink temperature shown in Fig. 1. Figure 7 delineates the resulting large thermal-runaway keepout region associated with these radiation heat-rejection conditions as defined by Eq. (6).

SUMMARY

It is well known that cryocooler thermal efficiency is a strong function of heat rejection temperature, roughly following the dependency described by Carnot. Measurements made on a variety of coolers indicate that this performance temperature sensitivity can be well modeled by an equation of the sort: $P_{T_2}(K) = P_{T_1}(K - [T_2 - T_1]/\mathfrak{R})$, i.e. the performance at cryogenic temperature K with a heatsink temperature T_2 is the same as that at heatsink temperature T_1 and cryogenic temperature $K - (T_2 - T_1)/\mathfrak{R}$, where \mathfrak{R} is a constant with a value in the range 2 to 7°C/K. This relationship has been used to develop a system-level cooler performance plot that displays the effect of the heat rejection temperature control mode on overall cryocooler performance. The plot also allows easy visualization of the stability boundaries and available stable operating space for the selected cooler and heat rejection control mode.

ACKNOWLEDGMENT

The work described in this paper was carried out by the Jet Propulsion Laboratory, California Institute of Technology and was sponsored by the NASA EOS AIRS Project through an agreement with the National Aeronautics and Space Administration.

REFERENCES

1. Ross, R. G., Jr. and Green, K. E., "AIRS Cryocooler System Design and Development," *Cryocoolers* 9, Plenum Publishing Corp., New York, 1997, pp. 885-894.
2. Smedley, G. T., Men, G. R., Johnson, D. L. and Ross, R. G., Jr., "Thermal Performance of Stirling-Cycle Cryocoolers: A Comparison of JPL-Tested Coolers," *Cryocoolers* 8, Plenum Publishing Corp., New York, 1995, pp. 185-195.
3. Johnson, D. L., Collins, S. A., Heun, M.K. and Ross, R. G., Jr., "Performance Characterization of the TRW 3503 and 6020 Pulse Tube Coolers," *Cryocoolers* 9, Plenum Publishing Corp., New York, 1997, pp. 183-193.
4. Burt, W.W. and Chan, C. K., "New Mid-Size High Efficiency Pulse Tube Coolers," *Cryocoolers* 9, Plenum Publishing Corp., New York, 1997, pp. 173-182.
5. Collins, S. A., Johnson, D. L., Smedley, G.T. and Ross, R. G., Jr., "Performance Characterization of the TRW 35K Pulse Tube Cooler," *Advances in Cryogenic Engineering*, Vol. 41, Plenum Publishing Corp., New York, 1996, pp. 1471-1478.